

# Applications of Multicore-Fiber Nonuniformly-Spaced Delay Lines in Microwave Photonics

Mario Annier González, Elham Nazemosadat and Ivana Gasulla

ITEAM Research Institute, Universitat Politècnica de València, Camino de Vera s/n, 46022 Valencia, Spain

[magonpe8@iteam.upv.es](mailto:magonpe8@iteam.upv.es)

**Abstract:** We experimentally demonstrate a flat-top bandpass microwave filter and a fractional Hilbert transformer in a multicore fiber. Both applications operate based on nonuniformly-spaced delay lines, providing equivalent negative tap coefficients by adjusting their time delays.

© 2024 The Author(s)

## 1. Introduction

Numerous microwave photonics signal processing functionalities rely on an incoherent approach that involves the combination of a set of time-delayed and amplitude-weighted replicas of an input radiofrequency signal. One of the primary constraints of such time-discrete processing structures lies in the difficulty of implementing negative or complex tap coefficients [1]. Among the variety of incoherent architectures reported so far [1], the use of nonuniformly-spaced delay lines brings interesting advantages [2]. Applying an adequate nonuniform time delay among neighboring taps leads to a  $\pi$  phase shift and provides an equivalent negative tap coefficient. This opens the way, for instance, to arbitrary frequency response filters while using all-positive tap coefficients. Up to date, different technologies have validated this method, such as the exploitation of wavelength diversity using a laser array along with phase-modulation to intensity-modulation conversion [2], or resorting to a chirped fiber Bragg grating [3].

The exploitation of space division multiplexing (SDM) in the context of time-discrete microwave signal processing has demonstrated to bring benefits in terms of compact parallelization and performance versatility [4,5]. In this work, by harnessing the spatial diversity inherent to a multicore fiber (MCF), we propose and experimentally demonstrate, for the first time, nonuniformly-spaced optical delay lines with direct application to two different microwave signal processing functionalities: a flat-top bandpass filter and a fractional/classical Hilbert transformer.

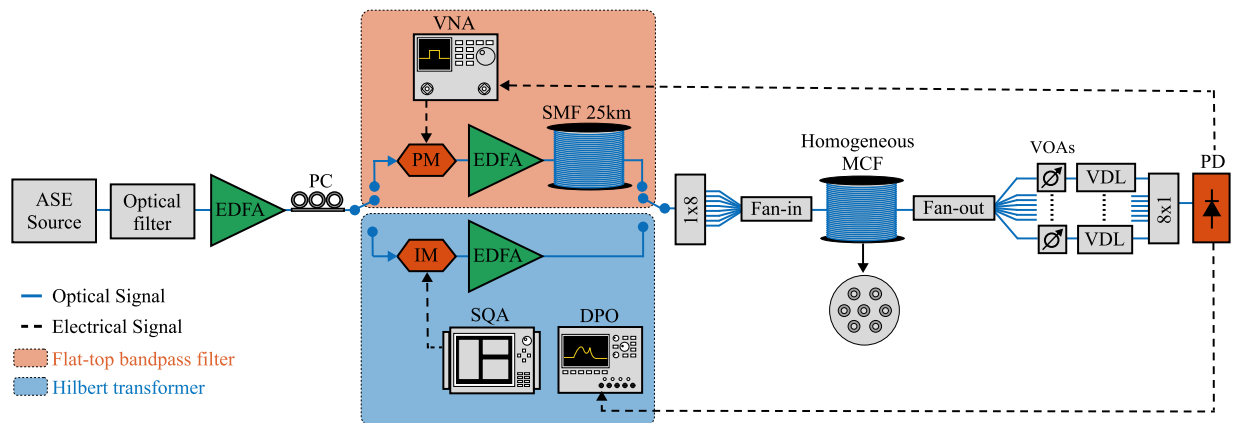


Fig. 1. Experimental setup for a flat-top bandpass filter and a Hilbert transformer based on a nonuniformly-spaced delay line microwave photonic filter. ASE: amplified spontaneous emission. EDFA: erbium-doped fiber amplifier. PC: polarization controller. IM: intensity modulator. PM: phase modulator. SMF: single-mode fiber. VOAs: variable optical attenuators. VDL: variable delay line. PD: photodetector. VNA: vector network analyzer. SQA: signal quality analyzer. DPO: digital phosphor oscilloscope.

## 2. Principle

We followed the design procedure outlined by [2] to transform uniformly-spaced true-negative coefficients into nonuniformly-spaced all-positive coefficients for two specific applications: a flat-top bandpass filter and a fractional Hilbert transformer (FHT). A FHT with a fractional order of  $\rho$ , applies a  $\pm\rho\pi/2$  phase shift around the central frequency of a signal, and has a unity magnitude response. In the case of  $\rho = 1$ , the FHT is referred to as a classical Hilbert transform (HT). We propose, for the first time, the use of a MCF to spatially multiplex the required signal samples, resorting for the experimental validation to the setup illustrated in Fig. 1. The approach involves propagating a modulated pulse along the cores of a 5-km homogeneous MCF (dispersion  $D = 17$  ps-nm/km at 1550 nm) and utilizing

external variable delay lines (VDLs) to adjust the time delay of the output signal replicas. The  $k^{\text{th}}$  replica of the output signal has an amplitude determined by the tap coefficient  $\beta_k$  and is spaced at an interval of  $\tau_k * T$ . Here,  $T$  represents the reference period, corresponding to a frequency filter (when combining all the samples together) with a free spectral range of  $1/T$ . The optical signal is generated by a broadband source and passed through a 0.2-nm-bandwidth optical filter. We employed variable optical attenuators (VOAs) to fine-tune the tap coefficient levels.

Initially, we constructed a filter with 11 taps, using the computed values of  $\beta_k = [0.127, 0, 0.18, 0, 0.636, 1, 0.636, 0, 0.18, 0, 0.127]$ , along with corresponding  $\tau_k = [0, 1, 2.5, 3, 4, 5, 6, 7, 7.5, 9, 10]$ . Our analysis reveals that four taps are zero-valued, suggesting the potential implementation of this filter with up to seven taps/cores. Besides, we introduced phase modulation (PM) and a 25-km standard single-mode fiber link to eliminate the baseband resonance.

Subsequently, we built a HT using  $\beta_k = [0.127, 0.212, 0.637, 0, 0.637, 0.212, 0.127]$ , spaced in time according to  $\tau_k = [-5.5, -3.5, -1.5, 0, 1, 3, 5]$ . Since the impulse response exhibits non-zero values for negative time intervals, for practical implementation, we employed the tap corresponding to  $\beta_{k=4}$  (the zero<sup>th</sup> tap) as a reference point in time and calibrated the system accordingly.

Finally, we implemented a FHT for fractional orders of 0.91, 0.7, 0.5, and 0.22. In this case, the zero<sup>th</sup> tap coefficients ( $\beta_{k=4}$ ), were adjusted to achieve the desired phase shifts, leading to  $\beta_{k=4} = [0.34, 0.99, 1.81, 4.85]$ , while the other taps were kept constant. Moreover, to evaluate the performance of the proposed system, we performed real-time FHT of a Gaussian-shaped pulse. This pulse was generated by a signal quality analyzer using a 128-digit binary sequence with only one bit being “1” (high voltage level) and a repetition rate of 90 MHz.

### 3. Experimental results

Fig. 2 shows the implemented microwave filter and HT using the MCF-based nonuniformly-distributed optical delay lines, with measurements obtained by a vector network analyzer. Figs. 2(a) and 2(b) depict the magnitude frequency response for a flat-top bandpass filter employing 5 and 7 taps/cores, respectively. The filters are centered at a frequency of 10 GHz (using  $T = 100$  ps), with bandwidths of 4.67 and 5.03 GHz, respectively. To facilitate comparison, we also present the ideal frequency response achieved with true-negative coefficients (uniformly-spaced samples, dotted-dashed yellow line) and all-positive coefficients (nonuniformly-spaced samples, dotted-dashed blue line). Both cases demonstrate a substantial attenuation of the baseband resonance, exceeding 30 dB. These results align well with the theory and previous experimental realizations using all-positive tap coefficients [2,6].

Figs. 2(c) and 2(d) illustrate the phase and magnitude frequency responses for a classical HT using seven taps/cores, which is configured to introduce the  $\pi$  phase shift at 8 GHz by setting  $T = 125$  ps for the first filter resonance. Similarly, we include theoretical representations for cases where true-negative and all-positive coefficients are utilized. The measurements agree well with theoretical predictions, showing a frequency response centered at 8 GHz with a bandwidth of 4.19 GHz and a phase shift close to  $180^\circ$ . The phase deviation within the bandpass is approximately  $\pm 1.7^\circ$  for the phase response; meanwhile, the normalized root mean squared error (NRMSE) for the magnitude is 14.52%. The system sensitivity to changes in the optical power level of each core leads to an error of above 10% in the magnitude. In both experiments, microwave signal processing was achieved utilizing nonuniformly-spaced delay lines by leveraging the spatial multiplexing capability within a MCF.

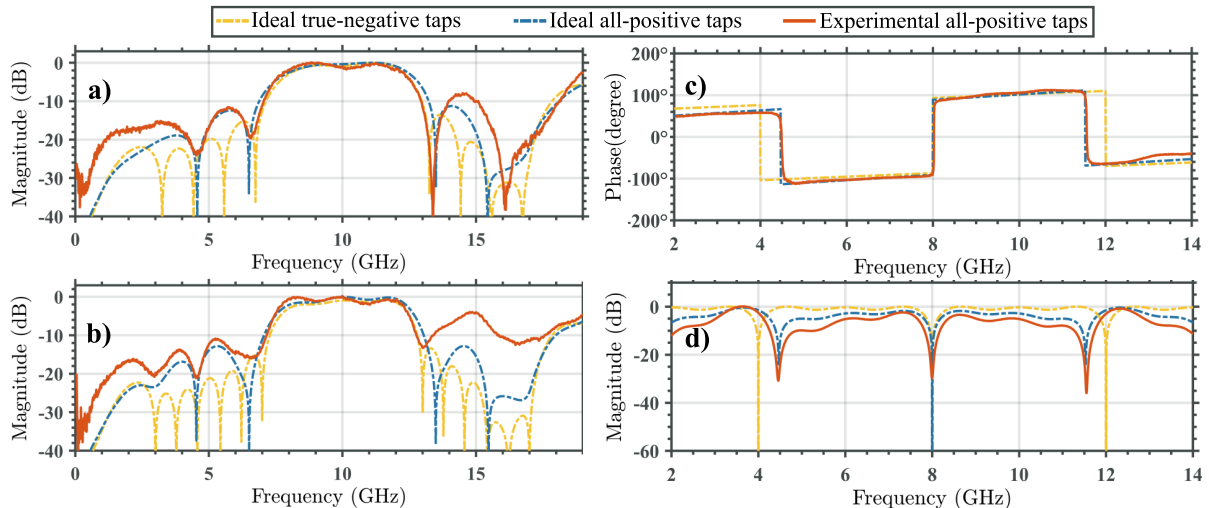


Fig. 2. Measured frequency response of nonuniformly-spaced applications compared to ideal counterparts: bandpass filter magnitude response when using (a) 7-cores and (b) 5-cores; Classical Hilbert transform using 7-cores: (c) phase and (d) magnitude responses.

Fig. 3 shows the experimental results (solid orange line) of the implemented FHT and their comparison with the theoretical simulation (dashed blue line). The phase frequency response of the FHT for fractional orders of 0.91, 0.7, 0.5, and 0.22 is shown in Figs. 3(a)-(d), respectively. The temporal amplitude FHT of the Gaussian pulse (input pulse in Fig. 3(e)), for fractional orders of 1.0, 0.87, and 1.22, are shown in Figs. 3(f)-(h), respectively.

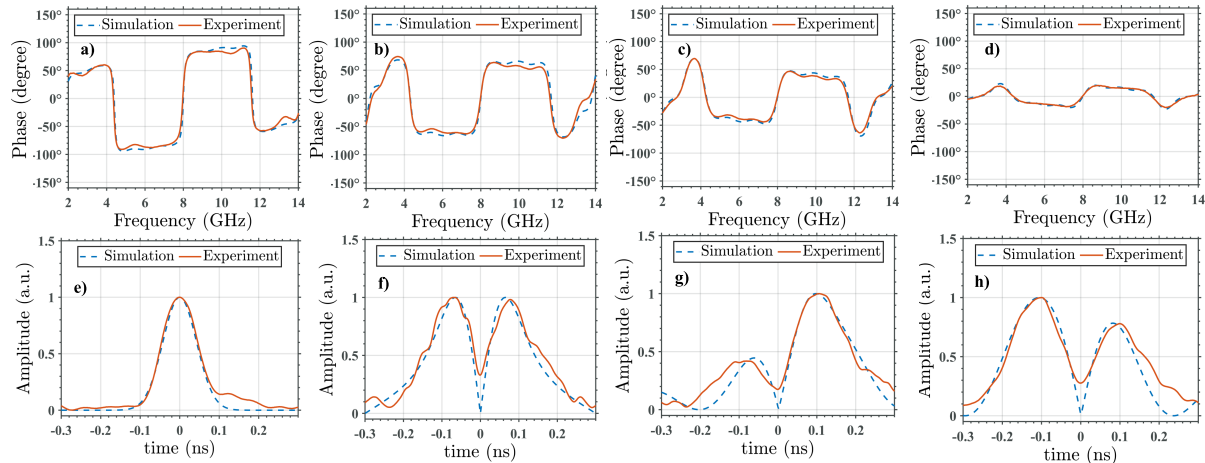


Fig. 3. Measured (orange) and simulated (dashed blue) phase and temporal FHT response. Phase response for fractional orders of (a)  $\rho=0.91$ , (b)  $\rho=0.7$ , (c)  $\rho=0.5$ , (d)  $\rho=0.22$ . (e) Input Gaussian pulse. Temporal FHT of the pulse for fractional orders of (f)  $\rho=1.0$ , (g)  $\rho=0.87$ , (h)  $\rho=1.22$ .

In the examination of phase responses within the 3-dB bandpass, for fractional orders of 0.91, 0.7, 0.5, and 0.22, we observe phase shifts of  $\pm 82^\circ$ ,  $\pm 63^\circ$ ,  $\pm 45^\circ$ , and  $\pm 20^\circ$ , with corresponding phase ripple of 4.76°, 3.54°, 3.33°, and 1.25°, respectively. These values lead to a maximum phase deviation of 2.38°, comparable to [7,8]. In terms of time response, the NRMSE between the measured and theoretical FHT pulses, for fractional orders of 1.0, 0.87, and 1.22, is 7.54%, 8.64%, and 11.04%, respectively, aligning closely with the findings presented in [6]. These figures indicate a strong agreement between the measured FHT phase and time responses and their theoretical predictions.

#### 4. Conclusions

For the first time to our knowledge, we experimentally demonstrated the feasibility of using nonuniformly-spaced delay lines for microwave signal processing exploiting the spatial diversity provided by a MCF. Specifically, we implemented two applications: a microwave flat-top bandpass filter with a bandpass centered at 10 GHz and fractional Hilbert transformer with different fractional orders, leading to a  $\rho\pi$  phase shift at 8 GHz. To test the behavior of our system furtherly, we also measured the temporal FHT of a Gaussian pulse. All in all, we proved the efficacy of SDM in simplifying the system architecture for time-discrete signal processing applications that require negative or complex coefficients. This demonstration extends the ability of MCFs to provide parallel optical and microwave signal processing while the signal is being distributed with increased compactness, therefore, eliminating the requirement for complex and challenging-to-implement structures. This strategy gains significance in scenarios where the presence of the fiber link is mandatory, such as, radio access networks for 5G and Beyond wireless communications.

#### 5. Acknowledgments

This work was supported by the ERC Consolidator Grant 724663, Spanish Ministerio de Ciencia e Innovacion project PID2020-118310RB-100 and fellowship PRE2021-099682, and Generalitat Valenciana PROMETEO/2021/15 project.

#### 6. References

- [1] J. Capmany, B. Ortega, y D. Pastor, "A tutorial on microwave photonic filters", *J. Light. Technol.* **24**, 201-229 (2006).
- [2] Y. Dai and J. Yao, "Nonuniformly Spaced Photonic Microwave Delay-Line Filters and Applications," *IEEE Trans. Microw. Theory Tech.* **58**, 3279-3289 (2010).
- [3] C. Wang and J. Yao, "A Nonuniformly Spaced Microwave Photonic Filter Using a Spatially Discrete Chirped FBG," *IEEE Photonics Technol. Lett.* **25**, 1889-1892 (2013).
- [4] I. Gasulla y J. Capmany, "Microwave Photonics Applications of Multicore Fibers," *IEEE Photonics J.* **4**, 877-888 (2012).
- [5] S. García, M. Ureña, and I. Gasulla, "Dispersion-diversity multicore fiber signal processing", *ACS Photonics* **9**, 2850–2859 (2022).
- [6] Z. Li, Y. Han, H. Chi, X. Zhang and J. Yao, "A Continuously Tunable Microwave Fractional Hilbert Transformer Based on a Nonuniformly Spaced Photonic Microwave Delay-Line Filter," *J. Light. Technol.* **30**, 1948-1953 (2012).
- [7] L. Zhuang, M. R. Khan, W. Becker, A. Leinse, R. Heideman and C. Roeloffzen, "Novel microwave photonic fractional Hilbert transformer using a ring resonator-based optical all-pass filter," *Opt. Express* **20**, 26499-26510 (2012).
- [8] M. Tan *et al.*, "Microwave and RF Photonic Fractional Hilbert Transformer Based on a 50 GHz Kerr Micro-Comb," *J. Light. Technol.* **37**, 6097-6104 (2019).